Title
Measurement of Oil and Gas Emissions from a Marine Seep

Authors
Leifer, Ira
Boles, J R
Luyendyk, B P

Publication Date
2007-03-14

Energy Development and Technology 009r

"Measurement of Oil and Gas Emissions from a Marine Seep"

Ira Leifer, Jim Boles, and Bruce Luyendyk

January 2007

Inquiries regarding this paper may be directed to Ira Leifer at ira.leifer@bubbleology.com

This paper is part of the University of California Energy Institute's (UCEI) Energy Development and Technology Working Paper Series. UCEI is a multi-campus research unit of the University of California located on the Berkeley campus.

UC Energy Institute
2547 Channing Way
Berkeley, California 94720-5180
www.ucei.org

New Energy Development and Technology (EDT-009) Working Paper January 2007[**]

Measurement of Oil and Gas Emissions from a Marine Seep

Ira Leifer[1], Jim Boles[2], and Bruce Luyendyk[2]

[1]Marine Science Institute, University of California, Santa Barbara, California, 93106.
[2]Department of Earth Sciences, University of California, Santa Barbara, California, 93106.

I. INTRODUCTION

Understanding the carbon flux across continental margins is of great interest due to their important role in global carbon budgets. Marine hydrocarbon seeps are found on all continental margins (*Judd et al.*, 2002) and are important to global atmospheric budgets of the important greenhouse gas, methane, contributing ~13% of natural emissions. In total, terrestrial and marine seeps are estimated to contribute 35-45 Tg yr^{-1} of methane (*Etiope and Klusman*, 2002), with approximately half arising from marine seeps (*Kvenvolden et al.*, 2001). Marine seep methane primarily arises from methane hydrates and thermogenic sources. Methane hydrates are a form of ice that is stable at high pressure and low temperature wherein methane gas is trapped in the ice crystal lattice. Methane hydrate deposits are estimated at 2000 Tg (*Collett and Kuuskraa*, 1998; *Kvenvolden*, 1999) and pose a significant climate threat should they destabilize and release their gas to the atmosphere. Thus, predicted oceanic warming due to enhanced greenhouse effect could cause this trapped methane to enhance atmospheric methane (*Kennett et al.*, 2003; *Leifer et al.*, 2006), causing a positive feedback. Yet, despite methane's importance to global climate atmospheric budgets, large uncertainty exists in the sources and sinks, and seeps as sources have been overlooked in most estimates of the global methane budget.

Marine seeps also are an important source of petroleum to the ocean. During the 1990s, natural seeps annually emitted an estimated 600,000 tons (150 million gals) of oil into the ocean, approximately half the annual total oil entering the ocean, ~1,300,000 tons. For comparison, spills from marine vessels accounted for 100,000 tons, terrestrial run-off, 140,000 tons, and

[**] Leifer, I., J. Boles, B. Luyendyk, 2007. Measurement of oil and gas emissions from a marine seep, *University of California Energy Institute Technical Report*, New Energy Development and Technology (EDT) Working Paper, EDT-009, Jan 2007.

pipelines just 12,000 tons. In North America, seeps emit an estimate of 160,000 tons (*NRC*, 2005).

To date, only a few quantitative emission rates have been published for seep gas emissions. Gas emission rates have been measured by sonar quantification (e.g., *Hornafius et al.*, 1999), turbine-tent flow measurements (*Leifer and Boles*, 2004), from a large seep tent (*Boles et al.*, 2001), and video-bubble emission measurements (*Leifer and MacDonald*, 2003). Even fewer quantitative measurements of seep oil emission rates have been published. Methods include estimation from oil slicks (*Clester et al.*, 1996), from a large seep tent (*Boles et al.*, 2001), and by direct capture from individual seep vents (*Leifer and Wilson*, 2004; 2006; *Mikolaj and Ampaya*, 1973). The latter studies showed an increase in oil emission with decreasing tidal depth. Further, in areas where oil and gas are emitted together, the presence of oil increases the challenge of measuring gas emissions – for example oil adheres to gas collection apparatus, and which can then become immobilized.

In this study, we developed and field-tested an approach to allow simultaneous quantification of both oil and gas emissions from shallow marine seeps in the Coal Oil Point seep field.

II. STUDY AREA – THE COAL OIL POINT SEEP FIELD

The Coal Oil Point hydrocarbon seep field is one of the largest known areas of active marine seepage and is conveniently located a few kilometers south from UCSB (Fig. 1). Several studies have quantified seep area (e.g., *Allen et al.*, 1970; *Fischer and Stevenson*, 1973) and emission fluxes (e.g., *Hornafius et al.*, 1999; *Quigley et al.*, 1999; *Clark et al.*, 2000) using sonar techniques, ocean chemistry, and direct gas capture with a floating buoys (*Washburn et al.*, 2001). During the last decade, the UCSB seep group has mapped the seep field using sonar and quantified seepage flux from sonar (*Luyendyk and Egland,* 2001*)* and direct gas capture using a flux buoy (*Washburn et al.*, 2001; 2005). Results indicate that ~1.5 x 10^5 m^3 day^{-1} (5 x 10^6 ft^3 day^{-1}) of seep gas is emitted to the atmosphere from ~3 km^2 of seabed (*Hornafius et al.*, 1999) with roughly an equal amount dissolved into the coastal ocean (*Clark et al.*, 2000).

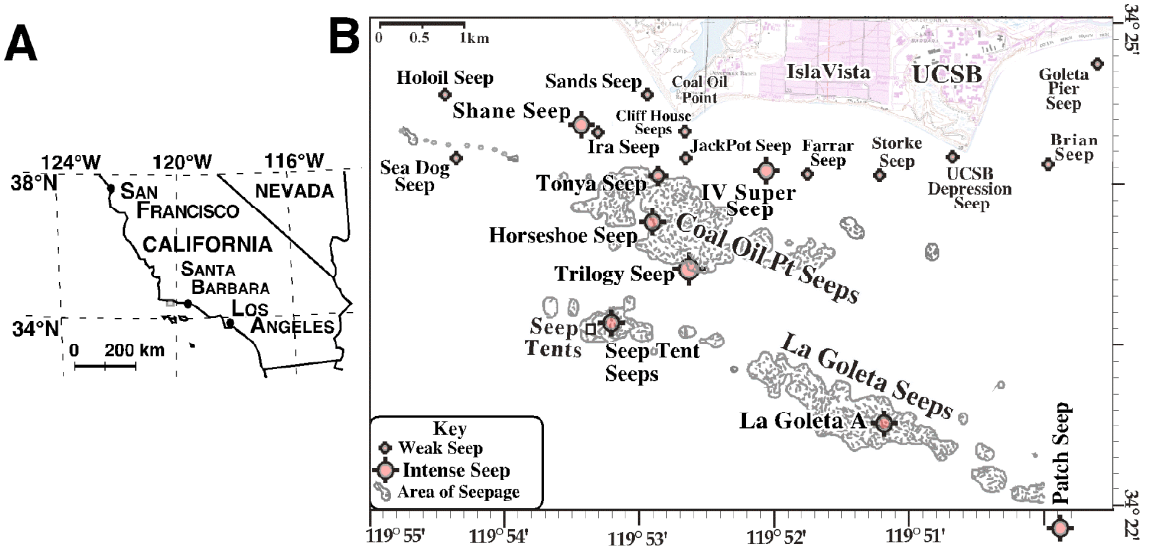

Fig. 1A. Overview map of S. California showing study area (small gray square). **B.** Map of the Coal Oil Point seep field. Informally named seeps shown by targets (target key and length scales on figure). Jackpot seep is to the south of Coal Oil Point. Gray areas are regions of high bubble density determined by sonar return (*Hornafius et al.*, 1999).

Most seepage is located along trends related to anticlines and associated fractures and faults. The inner trend is at ~20-m depth and includes the Farrar Seep, IV Super Seep,

Jackpot Seep, and Shane Seep. Depths are shallower south of the Coal Oil Point where the sea floor shows a slight rise. Jackpot Seep is at 15 m depth, the other seeps on this trend all are at ~20-m depth (Fig. 1). A second trend at ~40-m depth includes the Horseshoe and Coal Oil Point Seeps. The deepest trend is at ~70-m depth and includes the La Goleta and Seep Tent Seeps as well as Platform Holly. This trend corresponds to the intersection of the South Ellwood Fault with the ocean floor (*Fischer*, 1978). Seepage continues to occur along the S. Ellwood anticline trend despite recharging of sub-hydrostatic reservoir pressure by seawater moving down the fault (*Boles et al.,* 2004), indicating the flow is buoyancy driven along large fractures. There also is a very shallow trend of seepage in the vicinity of Coal Oil Point (Fig. 2), which is in a few meters water near Coal Oil Point, extending to approximately 5-m water to the western edge of the Sands Seeps. These shallow seeps emit only gas.

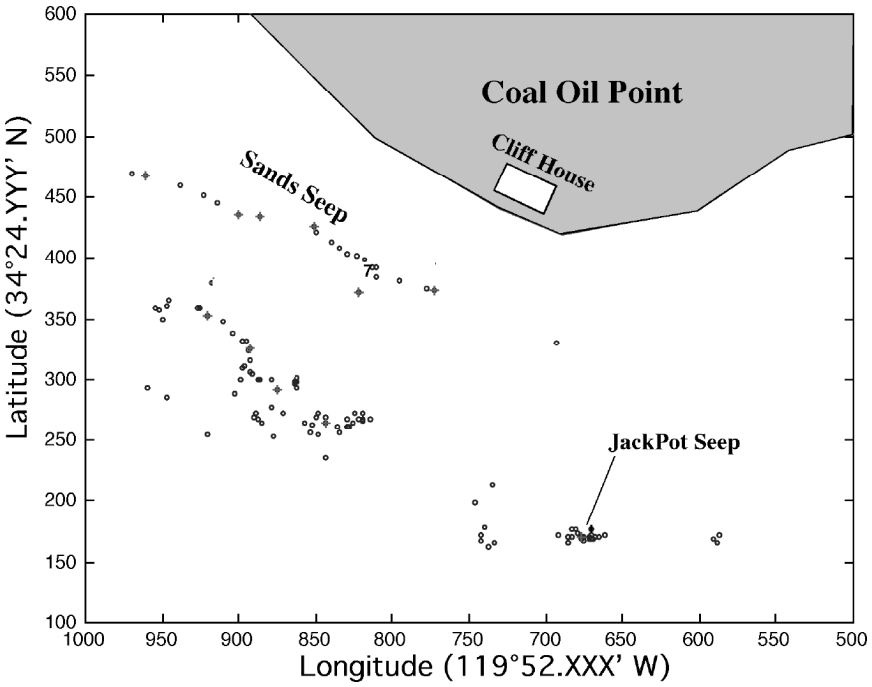

Fig. 2. Detail map of locations of seeps in the vicinity of Coal Oil Point, including the informally named Jackpot Seep and Sands Seeps. Targets are location of sighting of bubbles using GPS and do not reflect emission fluxes.

Seeps are quasi-permanent, depending on the time scale. For example, there is evidence that hydrocarbon seepage has been escaping from the basin margin for more than 100,000 years (*Boles et al.*, 2004) in areas at least 5-km north of the COP seep field. On decadal time scales, *Fischer and Stevenson* (1973) noted changes in hydrocarbon seeps in the Coal Oil Point area with a significant decrease in seepage areas between 1946 and 1973. Based on a comparison of sonar data and oil company seep maps, they attributed this drop to offshore production. Using data collected in 1973 and 1995, *Quigley et al.* (1999) demonstrated a decrease in the area and number of seeps within 1.5 km of Platform Holly that they attributed to production from the platform.

III. EXPERIMENTAL APPROACH

III.A. Tent Design

The tent design is an adaptation of the turbine seep tent, described in *Leifer and Boles* (2005) and shown in Fig. 3. Modifications include attaching stainless-steel foil to the tent interior, insertion of an oil-gas separator between the tent and the turbine, and a new data encoder for the turbine.

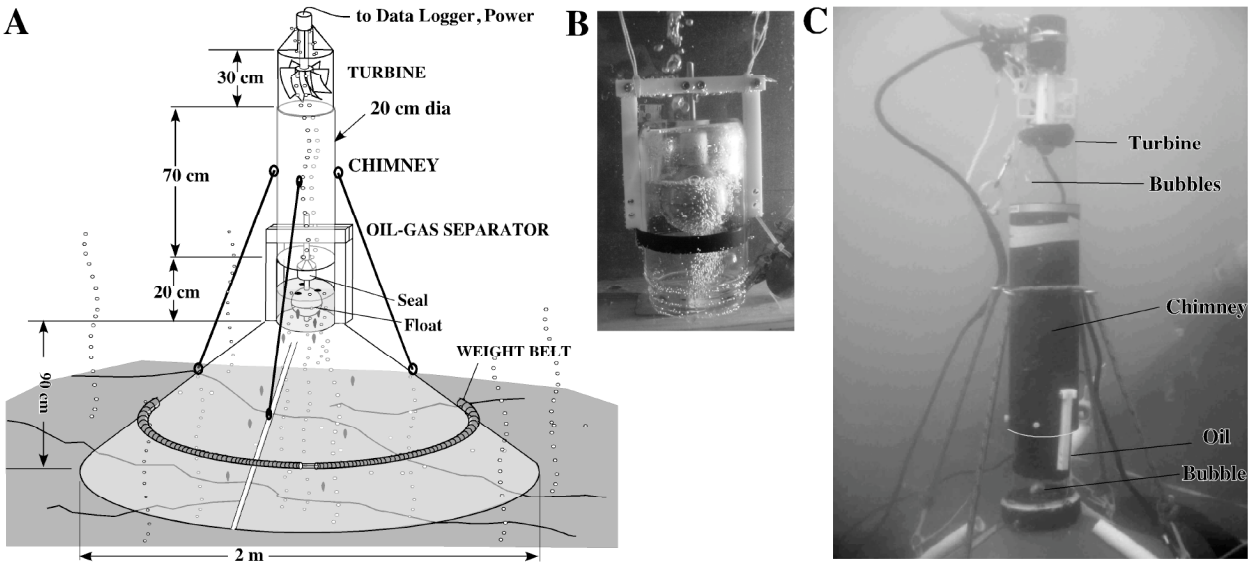

Fig. 3A. Schematic of the seep tent, oil-gas separator, and gas flux turbine. **B.** Image of oil-gas separator in the laboratory without the tent. **C.** Underwater image of field deployment, photo courtesy Tonya Del Sontro (UCSB).

The seep tents are formed from 1/8-inch PVC sheets pop-riveted into a 2-m diameter, 1-m tall, inverted cone. A support frame of 1/2-inch diameter PVC plastic pipes was riveted exterior of the tent for attachment of the deployment bridle and weights. The frame consisted of a hoop at the tents bottom edge and four spars up the sides. The bottom frame hoop was attached to the tent by a rope threaded through a series of holes at the tent's bottom edge. The deployment bridle was attached to three eyebolts through the support spars. Instead of weights as used previously, a weight belt constructed of vacuum hose filled with lead with quick release belts attached to the ends was used. This provided a uniform weight distribution, allowing SCUBA divers to more

easily add/remove weight to the tent, in greater quantity than the previous approach of attaching weights to the bottom hoop. Weight belts were ~20 kg. To prevent swell-induced water motions in from entering under the tent and spinning the turbine, it was important that the weights pressed the tent flush or into the seabed. For this deployment, two SCUBA weight belts were used.

Another important modification was covering the tent's inside surface with stainless-steel foil (0.05-mm thick), which was pop-riveted to the tent. Gaps in the foil coverage were covered with stainless-steel tape (0.05-mm thick). The foil allowed the inner surface to be washed with the solvent dichloromethane (DCM) after tent retrieval to recover oil that had adhered to the tent's inner surface during deployment. A cutoff stainless-steel funnel was inserted in the apex of the tent. The funnel was cut to slightly smaller than the diameter of the oil-gas separator, which used a 1000-ml sample jar. A collar was silconed to the outside of the tent at its apex. A sample-jar cap, which had a hole slightly larger than the funnel opening cut into it, was epoxied into the tent collar. This allowed the oil-gas separator to be threaded into the tent collar, eliminating the need for the retention straps used in a previous version of the oil capture tent. Stainless-steel bolts were threaded into the collar to help align the sample jar. A small video camera was mounted on the seep tent to monitor the sample jar and alert shipboard scientists as the jar began to fill.

An oil-gas separator was developed in an inverted 1-liter sample jar. It consisted of a stainless-steel float and a Teflon seal, both of which were mounted on a rod. The rod was secured in a Delron^{TM} frame that was secured to the jar. The float and seal could move freely up and down on the rod. The top of the seal was beveled at a 30° angle and matched a beveled hole in the top of the sample jar. When the jar was filled with water, the float pushed the seal into the hole and sealed the jar. As gas entered the jar, the water-gas interface layer descends and the buoyancy force on the float decreases. When the interface drops below approximately 10 cm, the hole unseals and gas escapes. The escaping gas causes the gas-water interface to rise and the seal re-closes the hole, trapping the gas. As a result, the interface varies between 9 and 10 cm below the jar top for a slow flux, and oil accumulates at the interface and cannot escape the jar. For higher flux, the interface is closer to the exit hole.

A chimney tube with four stabilizing tension lines connected the turbine to the oil-gas separator and provided time for the rising bubbles escaping the separator to accelerate the surrounding water and form the upwelling flow that spins the turbine. The stabilizing lines were adjusted in the field to ensure that the turbine and chimney tube were vertical. For the deployment described here, the chimney tube was black plastic; future deployments will use clear acrylic to allow inspection of the oil-gas separator.

The turbine was machined out of a polyvinyl chloride (PVC) block with 4 blades tilted at 45°. As a result, all vertical paths through the turbine (i.e., that of rising bubbles) intersect a blade surface. The turbine is mounted securely in the chimney and with its outer blade edges parallel to the chimney wall with clearance of approximately 1 mm. The chimney was clear acrylic to allow visual inspection of the turbine, thereby assuring that it was not debris blocked (primarily a concern during deployment). The turbine had a 2-cm diameter central axle with internal glass bearings in ultra high molecular weight (UHMW) plastic races to minimize friction without lubrication. In *Leifer and Boles* (2005), the turbine spin rate was recorded by a data logger with pulses formed by a Hall effect sensor. The four blades contained small magnets, which yielded four pulses per second. To improve the time resolution an optical encoder created pulses with 100 pulses per rotation. The data logger (OMP-MODL, Omega Corp, CT) counted the number of pulses per time unit, where the user can choose the time interval.

III.B. Laboratory Calibration

The flow as a function of rotation rate was calibrated in the laboratory in the Ocean Engineering Laboratory wind-wave channel (5-m wide by 3-m deep by 42-m long) and the flow, F ($cm^3\ s^{-1}$), was well-fit to the pulse rate, P (Hz), by an approximately quadratic function,

$$F = 0.0023\ P^{2.059} \qquad (1)$$

over the range $5 < F < 10^3$ $cm^3\ s^{-1}$, which spanned the field data (Fig. 4). For $F \leq 5$ $cm^3\ s^{-1}$, gas emissions from the separator were intermittent and did not always persist sufficiently long enough to overcome inertia and start the turbine spinning.

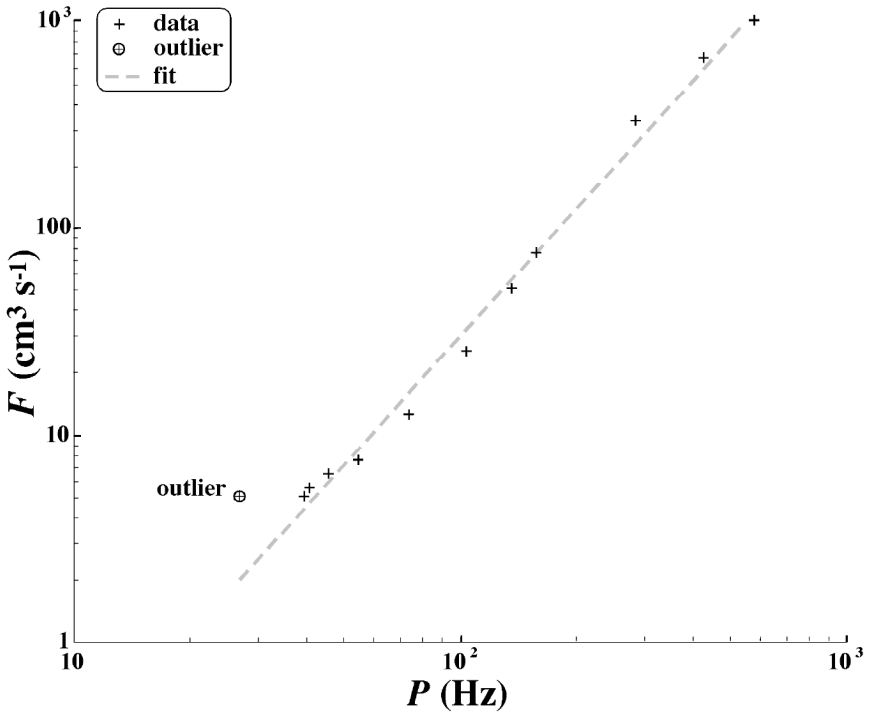

Fig. 4. Laboratory calibration data and linear least squares regression analysis fit of flow rate, *F*, versus pulse rate, *P*, for set-up in Fig. 3. Flow is at STP, the turbine was at a depth of ~2 m. Circle represents where for *F*, inertia becomes significant and was not used in the fit. Data key is on figure.

IV. FIELD DEPLOYMENT

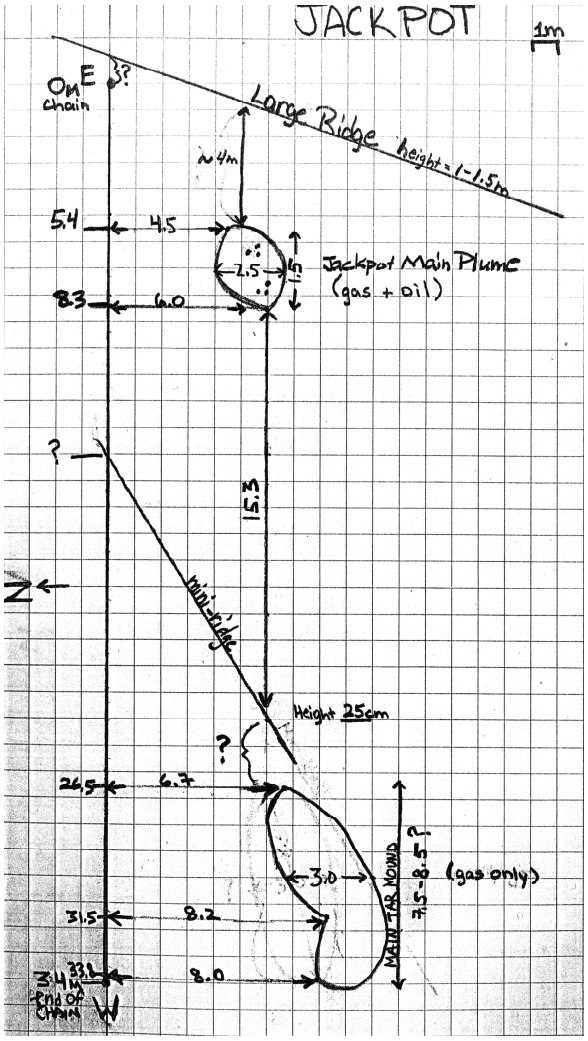

Fig. 5. Map of Jackpot Seep based on a series of scuba dives. North is to left. Large ridge at the map top is about 1 to 1.5 m tall.

A preliminary field deployment of the oil-gas separator without the tent was made on 11 Oct. 2006 for 6 minutes 15 seconds at 10:10 Local Time (LT) during a +1.5-m tide. The system also was deployed at Jackpot Seep on 16 Nov. 2006 at 10:51:14 LT for approximately 90 minutes. Jackpot Seep is in approximately 14-m water located at the northern edge of an outcropping of the Monterey Formation, and is the shallowest oily seep in the COP seep field (Fig. 1). As the shallowest, diver accessible seep, Jackpot Seep provides the longest bottom time for SCUBA divers. Jackpot Seep has been active for several decades at least – it was surveyed by Alan A.

Allen (personal communication) in 1969. However, the oil emissions from the COP seep field reported in *Mikolaj and Ampaya* (1973) may have been from the IV Super Seep area (Fig. 1). Although site descriptions in *Mikolaj and Ampaya* (1973) more closely match those currently observed at Jackpot Seep than IV Super Seep, a map in *Mikolaj and Ampaya* (1973) suggest their measurements were at or near IV Super Seep.

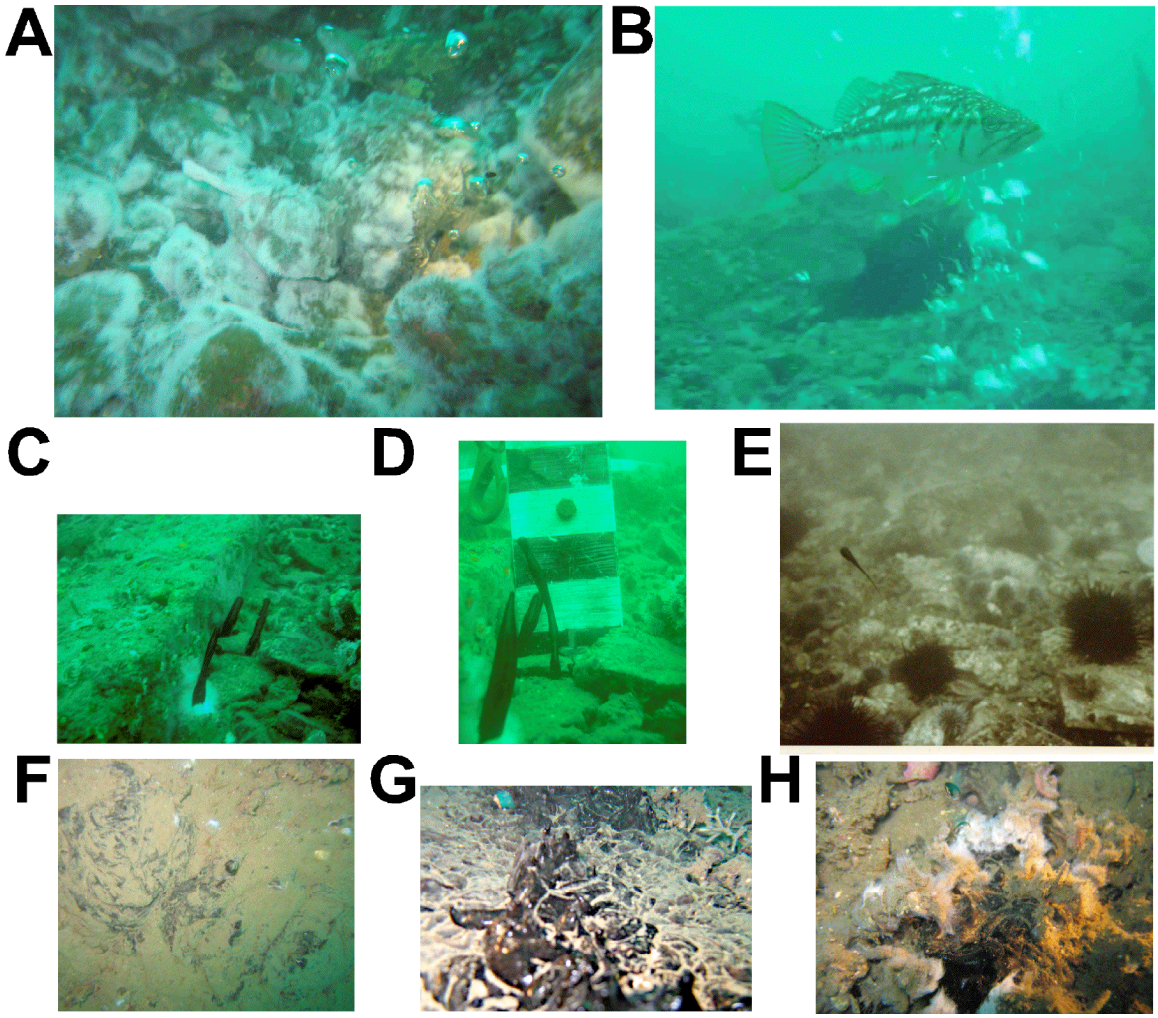

Fig. 6. Photos of Jackpot Seep at the seabed. **A** and **B** are of the main vent. **C** and **D** are of oil emissions from near the low ridge labeled "mini ridge" in Fig. 5. **E** is a photo of Jackpot seep taken in 1970 showing a tar streamer. Precise location in the seep field is unknown. **F – H** are of the western edge of Jackpot seep area where the tar mounds are. Photo **E** is courtesy of Alan A. Allen; other photos courtesy of Tonya Del Sontro, UCSB.

Vents associated with Jackpot Seep are spread over a linear east-west trend stretching approximately 20 m, with the main vent site confined to an area approximately 2 m across (Fig. 5). The seabed is cobble and sand (Fig. 6A), and there were a number of large rocks in the vicinity of the main vent during the deployment. These rocks were relocated by SCUBA divers to allow the tent to sit flush on the seabed. The site is about 5 m from a pronounced ridge, approximately 1 to 1.5 m high, which follows a roughly linear north-south trend. Approximately 10 m to the west of the main vent lies a small ridge (Fig. 5) along which small tar whips (to several centimeters) were observed (Figs. 6C & D). At the western edge of the Jackpot Seep were exposed asphalt flows (above the sediment), which exhibit layered structure. From these flows, short tar whips also were observed (Figs. 6F-H). This corresponds to descriptions of Jackpot Seep over thirty years earlier by Alan A. Allen (personal communication, 2005).

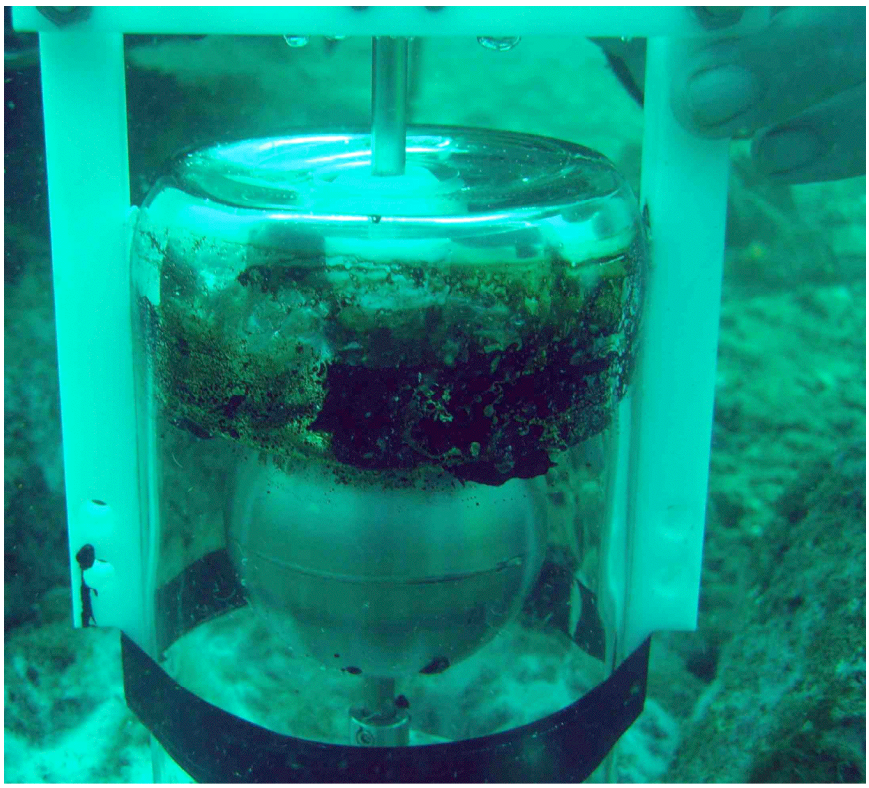

Fig. 7. Photo of preliminary test of oil-gas separator at main vent of Jackpot Seep.

During the preliminary deployment, the oil-gas separator was held over a 30-cm diameter funnel at the main vent for several minutes to estimate the oil flux emission rates in preparation for the field study. Four scuba divers captured gas in a series of 1-liter glass bottles, which allowed estimation of gas emission rates. Each bottle was allowed to fill, and then a diver recorded the elapsed time for the bottle to fill, as another bottle was swapped over the funnel mouth. This process was continued for approximately five minutes. Gas emissions were ~100 cm^3 per minute, during which one to two milliliters of oil was collected in one of the bottles (Fig. 7). Also, a gas pulse was observed during the bottle swap during which gas flux was much larger than the average, demonstrating the variability in emissions.

Samples of gas from Jackpot Seep were collected on 29 Nov. 2004 and 26 April 2006 and analyzed (courtesy Frank Kinnaman, UCSB). The gas was predominantly methane, 84%, with the next most common gas, carbon dioxide at 14%. In the samples, nitrogen was trace, at 0.54%; n-alkanes C2-C4 were identified, with more propane (0.63%) than ethane (0.30%). Finally, butane was observed at 0.19%. The fraction of methane and carbon dioxide are comparable to observations for Shane Seep to the west (Fig. 1). As the bubbles rise, the carbon dioxide rapidly outflows the bubbles, while the air gases inflows, such that by the time bubbles reach the sea surface, the carbon dioxide is reduced to trace amounts, and the air gases have increased significantly.

V. DATA ANALYSIS AND RESULTS

Using Eqn. (1), F was calculated from the field data. For the first hour, the mean F was 12.6±13.3 cm^3 s^{-1} (Fig. 8), with a sudden increase at approximately 1210 local time (LT). Total gas emissions over the deployment time were 64 liters at the seabed, or 150 liters at standard temperature and pressure (STP). Based on laboratory studies, interactions between oil and gas in the separator affected emissions on time scales of 0.25 s or slower and for lower emission rates, F < 10 cm^3 s^{-1}). Emissions were highly unsteady, ranging from zero to as high as 100 cm^3 s^{-1}. Shortly after 12:00 LT, emissions increased dramatically accompanied with significantly greater variability. At this point, the jar rapidly began filling with oil and the divers were mobilized to hurriedly retrieve the sample jar before it could overflow. Underwater video showed that the variability coincided with submergence of the entire float and part of the seal in oil. Thereafter, gas bubbles were forced to rise through a thick layer of oil, while previously, gas-free pathways were observed through the oil layer.

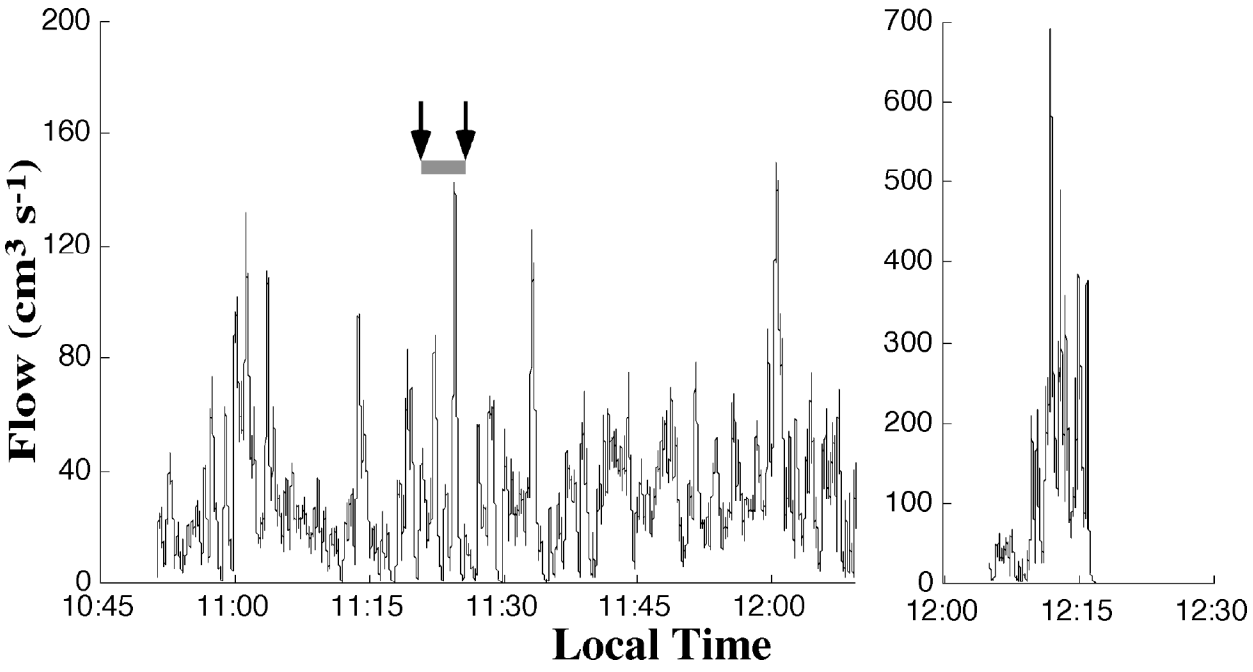

Fig. 8. Field emission data. Data were low-pass filtered with a 1st order Butterworth filter with cutoff frequency at 50 s. Arrows show location of segment shown in Fig. 4. Note, last fifteen minutes of data have different vertical axis.

Frequently, gas emissions were pulsed with the turbine showing that emissions sporadically ceased for periods of several seconds. An example is shown in Fig. 9A for a 220-second time series beginning 11:21:36 LT. Examination of the video showed that emissions into the oil-gas separator generally were more or less continuous, although they infrequently ceased for periods of 0.25 to 0.5 s. The video also showed that the emissions were pulsed, with periods of relative quiescence and periods of great activity. Further, during an emission pulse, the data show variability with a periodicity of ~5 seconds – e.g., at 150 s in Fig. 9A. Fourier spectral analysis is inappropriate because observations only can occur during short pulses when the oil-gas separator remained largely open and continuously fluxing. To analyze the data, the Burg spectral approximation method was used to calculate a *spectragram* (*Leifer and Tang*, 2006), shown in Fig. 9B. During the pulse at 175 s, there was a distinct peak at a period of approximately 5 s. A similar peak at approximately 5.5 s period was observed during the pulse at 25 seconds. The average spectrum for this data subset is shown in Fig. 10 and shows a clear peak at approximately 5.3 s.

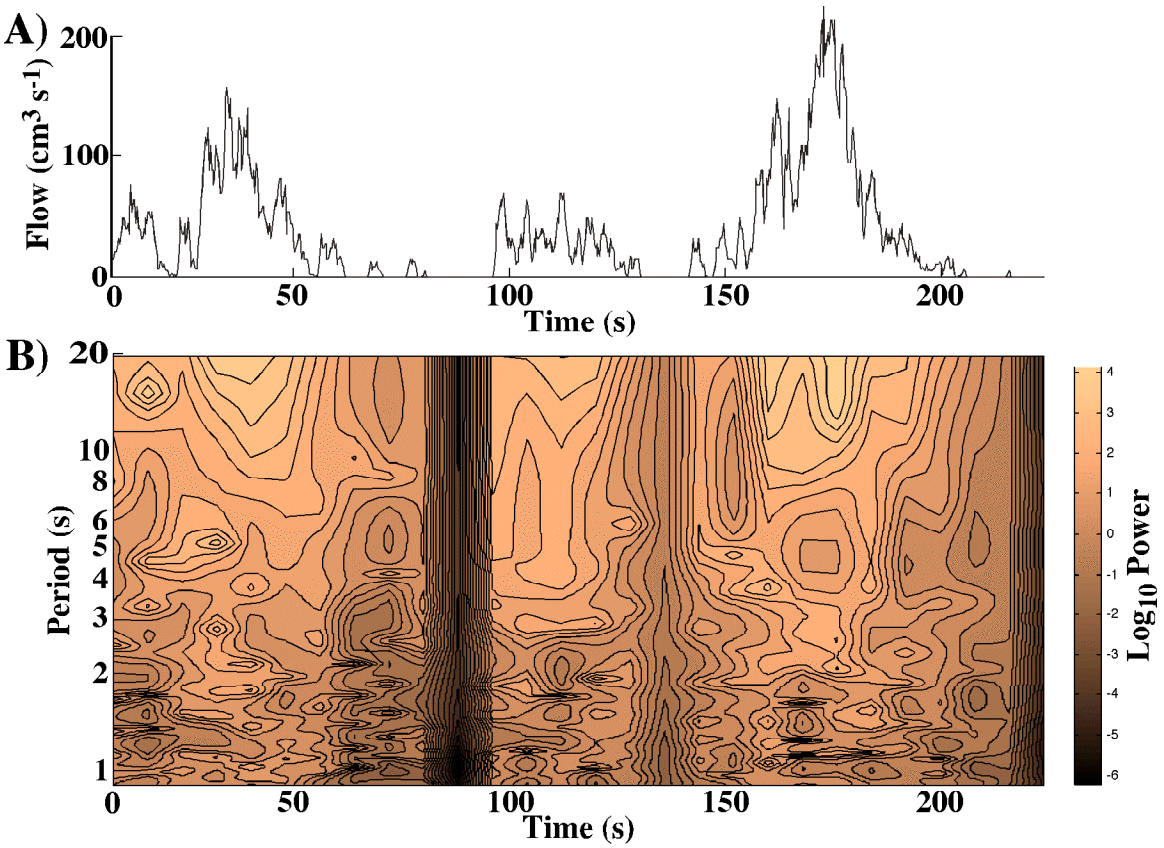

Fig. 9A. Data subset starting at 11:21:36**. B.** Spectragram calculated by a 1024-pt, 32-pole Burg spectral approximation method with for 16-s data subsets, with overlap of 25%, and a Hanning window.

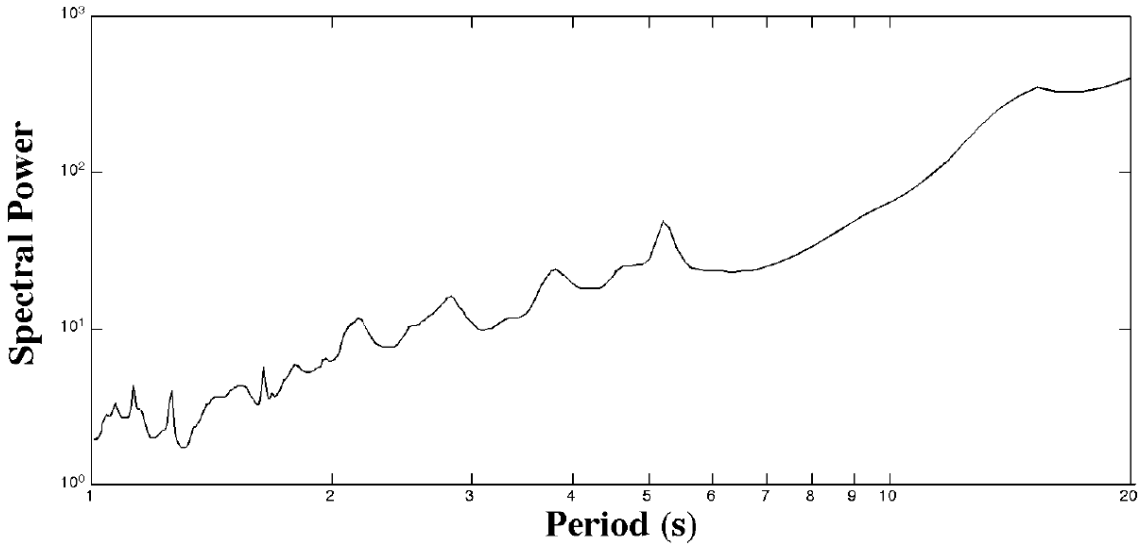

Figure 10. Average spectra for data shown in Fig. 9.

Calculation of the spectra for the first hour of the data set (Fig. 11) shows a peak in the range 5 to 7-second period and a trough at 8-second period. The periods of peaks and troughs correspond to the wave spectra recorded at the West Santa Barbara Channel NOAA Buoy.

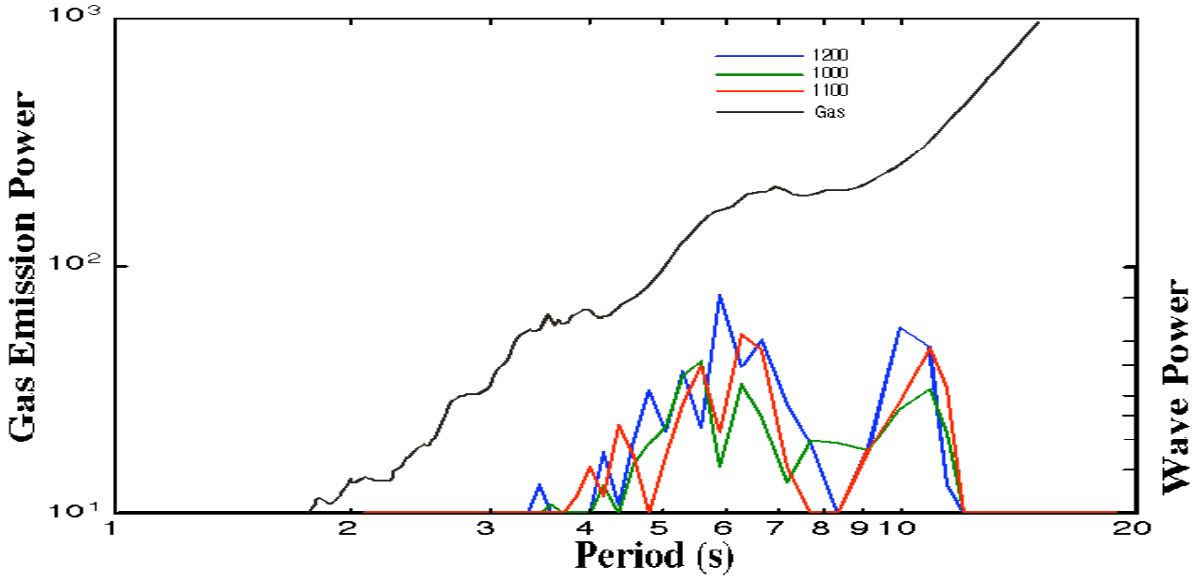

Fig. 11. Spectra from the turbine flux data and wave data at 10:00, 11:00 and 12:00 local time. Data key on figure.

Further, the gas pulse showed structure at several time and flux scales. Short-lived pulses of approximately 1 second were observed every five or six seconds during the event, and likely were related to swell, which had a period of 5 to 6 s. These pulses last approximately one or two seconds – i.e., significantly longer than the bubble transit time through the turbine (0.2 s). Because groups of seep bubbles often are observed escaping together at the seabed (*Leifer and Tang*, 2006), the data indicate that seepage likely was in groups or pulses of bubbles.

After deployment, the oil-gas separator was stored for several days to allow the oil and water to separate. The water was then decanted, and the collected oil and the oil-gas separator was weighed. To determine the amount of oil collected, the oil was then removed from the separtor with a solvent, and the empty oil-gas separator was weighed. Thus, it was found that a total of 164 g oil was collected over 95 minutes. After the deployment, there was no oil on the turbine. Oil from the stainless-steel foil lined tent was rinsed into a sample jar with dichloromethane. Total gas emissions over the deployment were 150 liters at standard temperature and pressure, yielding a gas to oil ratio of 920 to 1by volume. Analysis of the video camera images of the oil gas separator during oil collection at the seabed showed that oil accumulation was highly uneven.

VI. CONCLUSION AND FUTURE EFFORTS

The oil-gas separator deployed was the result of improvements made on several unsuccessful prototypes. Measured, oil emission rates were near the maximum acceptable for the design oil-gas separator. Further, analysis of the video showed that even over the approximately 1 hour deployment, oil emission rates were highly variable. Visual observations suggested that trace oil was collected from primarily gassy bubbles (Fig. 6B); however, every few seconds to tens of seconds, very oily (appearing black) bubbles were observed often with an oil streamer or tail (Fig. 6E). Thus, oil emissions were orders of magnitude greater whenever an oil streamer escaped. These very oily bubbles mostly escaped from different sites at the seabed than where clear bubbles primarily escaped; with all sites located within a few centimeters. Oil accumulation under rocks and/or openings in the sediment and cobble may have played a role in the location of the emission sites for oily bubbles. Also, emission rates were several orders of magnitude greater during the full deployment than during the preliminary deployment. However, the tent covered a much larger area of seabed in the second deployment and thus more vents than the funnel used during the preliminary deployment. Unfortunately, a simple area scaling-factor cannot be used to compare the two experiments because the spatial distribution of vents at the seabed is not gaussian or uniform. Thus, the measured oil emission rate may be unrepresentative of Jackpot Seep emissions. Nevertheless, this represents the first and only simultaneous measurement of oil and gas emissions from a natural marine seep.

The original deployment plan was to deploy the oil-gas separator, then retrieve it to the boat, dissolve the oil in the oil-gas separator with dichloromethane into a sample jar for later analysis, and then redeploy the oil-gas separator. This plan would have provided a time series of oil and gas emission rates that could be related to tidal depth. This approach would have been feasible for oil emission rates of a few milliliters per minute, as during the preliminary deployment, but not for the much greater emission rate during the full deployment. To successfully study emissions at these higher flux rates will require several oil-gas separators.

Combining the oil-gas separator with the turbine tent demonstrated a second important benefit of the oil-gas separator – as a protector of the turbine from oil. Absent the oil-gas separator, the turbine would have accumulated significant oil on its blades and then would have rapidly

decreased its efficiency – i.e., changed its calibration curve. Eventually, the turbine would become completely clogged and stop working. However, after the field deployment, the turbine was completely oil free – i.e., the oil-gas separator had fully protected the turbine from the oil. Thus, an oil-gas separator with an exit port is a critical step towards successful long-term deployment of a turbine-tent network.

Based on the original UCEI turbine tent proposal, funds were awarded from the American Chemical Society (ACS) for the development and deployment of an 8-tent turbine-tent network. Under the ACS project, a second oil-gas separator has been built and a deployment is planned for late spring 2007. Also, interpretation of the temporal response of the turbine under conditions of pulsing as observed at Jackpot Seep–which was not observed during the turbine-tent deployment at Shane Seep (*Leifer and Boles*, 2005) – requires a series of laboratory calibration experiments for a pulsing gas source. These calibration experiments currently are being conducted under the ACS project. Also being conducted is a series of experiments to determine the temperature sensitivity in the turbine response, and the sensitivity to salinity.

VII. REFERENCES

Allen A.A., R.S. Schlueter, and P.G. Mikolaj, Natural oil seepage at Coal Oil Point, Santa Barbara, California. *Science* **170**, 974-977, 1970.

Boles, J.R., J.F. Clark,, I. Leifer, and L. Washburn. Temporal variation in natural methane seep rate due to tides, Coal Oil Point area, California. *J. Geophys. Res.* **106 C11**, 27077-27086, 2001.

Boles J.R., P. Eichhubl, G. Garven, and J. Chen, Evolution of a hydrocarbon migration pathway along a basin bounding fault: Evidence from fault cements. *AAPG Bulletin*, **88**, 947-970, 2004.

Clark J.F., L. Washburn, J.S. Hornafius, and B.P. Luyendyk, Dissolved hydrocarbon flux from natural marine seeps to the southern California Bight. *J. Geophys. Res.* **105**, 11509-11522, 2000.

Clark, J.F., I. Leifer, L. Washburn, and B.P. Luyendyk, Compositional changes in natural gas bubble plumes: Observations from the Coal Oil Point marine hydrocarbon seep field, *Geo-Marine Letters* **23**, 187-193 DOI 10.1007/s00367-003-0137-y, 2003.

Clester, S.M., J.S. Hornafius, J. Scepan, and J.E. Estes, Quantification of the relationship between natural gas seepage rates and surface oil volume in the Santa Barbara Channel, (abstract), *EOS (American Geophysical Union Transactions)* **77 46)**, F419, 1996.

Collett, T.S., and V.A. Kuuskraa, Emerging US gas resources; 4, Hydrates contain vast store of world's gas resources, *Oil and Gas Journal* **96(19)**, 90-95, 1998.

Etiope, G., and R.W. Klusman, Geologic emissions of methane to the atmosphere, *Chemosphere* **49(8)**, 777-789, 2002.

Fischer, P.J., Natural gas and oil seeps, Santa Barbara Basin, California. In *California Offshore Gas, Oil, and Tar Seeps*, (pp 1-62). State Lands Commission Report, 1978.

Fischer P.J., and A.J. Stevenson, Natural hydrocarbon seeps, Santa Barbara basin, California, Santa Barbara Channel area revisited. Ed. Fischer PJ, *Field Trip Guidebook*, *Volume 3* (pp. 17-28). American Association of Petroleum Geology, Tulsa, OK, 1973.

Hornafius, J.S., D.C. Quigley, and B.P. Luyendyk, The world's most spectacular marine hydrocarbons seeps (Coal Oil Point, Santa Barbara Channel, California): Quantification of emissions, *J. Geophys. Res. Oceans* **104 (C9)**, 20703-20711, 1999.

Hovland, M., J. Gardner, and A. Judd, The significance of pockmarks to understanding fluid flow processes and geohazards, *Geofluids* **2**, 127-136, 2002.

Judd, A.G., M. Hovland, L.I. Dimitrov, S. Garcia Gil, and V. Jukes, The geological methane budget at continental margins and its influence on climate, *Geofluids* **2**, 109-126, 2002.

Kennett, J.P., K.G. Cannariato, I.L. Hendy, and R.J. Behl, *Role of Methane Hydrates in Late Quaternary Climatic Change: The Clathrate Gun Hypothesis*, 216 pp., American Geophysical Union, 2003.

Kvenvolden, K.A., Potential effects of gas hydrate on human welfare, *Proceedings of the National Academy of Sciences of the U.S.A.* **96 (7)**, 3420-3426, 1999.

Kvenvolden, K.A., T.D. Lorenson, and W.S. Reeburgh, Attention turns to naturally occurring methane seepage, *EOS (American Geophysical Union Transactions)* **82**, 457, 2001.

Leifer, I., and K. Wilson,. Tides and the emission of oil and gas from an abandoned oil well: Nearshore, Summerland, California. *Mar. Poll. Bull., Submitted*, 2006.

Leifer, I., and K. Wilson, Quantified oil emissions with a video-monitored, oil seep-tent. *Marine Technology Society Journal* **38 (3)**, 44-53, 2004.

Leifer, I., and D.J. Tang. The acoustic signature of marine seep bubbles, *J. American Society of Acoustics Express Lett.* **121(1)**, EL35-EL40, *doi:10.1121/1.240122*, 2006.

Leifer, I., and I.R. MacDonald, Dynamics of the gas flux from shallow gas hydrate deposits: Interaction between oily hydrate bubbles and the oceanic environment, *Earth and Planetary Science Letters* **210**, 411-424, 2003.

Leifer, I., and J.R. Boles, Turbine tent measurements of marine hydrocarbon seeps on subhourly time scales, *J. Geophys. Res.,* **110**, C01006, doi:10.1029/2003JC002207, 2005.

Leifer, I., B. Luyendyk, J. Boles, and J.F. Clark, Natural marine seepage blowout: Contribution to atmospheric methane. *Global Biogeochemcial Cycles* **20(3)**, doi:10.1029/2005GB002668, 2006.

Luyendyk, B., and E.T. Egland, Variation in discharge from marine hydrocarbon seeps at Coal Oil Point, CA: Implications for offshore oil production, Final report for University of California Energy Institute CES grant FY 1999-2000, Contribution of the Institute for Crustal Studies Number 418-137TC, 42 pages, 2001.

Mikolaj, P.G., and J.P. Ampaya, Tidal effects on the activity of natural submarine oil seeps. *Marine Technology Society Journal* **7**, 25 – 28, 1973.

NRC (National Research Council). Oil in the sea III: Inputs, fates and effects, National Academy Press, Washington, D.C., pp 265, 2003.

Quigley, D.C., J.S. Hornafius, B.P. Luyendyk, R.D. Francis, J.F. Clark, and L. Washburn, Decrease in natural marine hydrocarbon seepage near Coal Oil Point, California associated with offshore oil production, *Geology*, **27(11)**, 1047-1050, 1999.

Washburn, L., C. Johnson, C.C. Gotschalk, and E.T. Egland, A gas-capture buoy for measuring bubbling gas flux in oceans and lakes. *J. Atmos. Ocean. Tech.* **18(8),** 1411-1420, 2001.

Washburn, L., J.F. Clark, and P. Kyriakidis, The spatial scales, distribution, and intensity of natural marine hydrocarbon seeps near Coal Oil Point, California, *Marine and Petroleum Geology* **22(4)**, 569-578, 2005.